Electronic Supplementary Information

Integration of Mo$_2$C-embedded nitrogen-doped carbon with Co encapsulated in nitrogen-doped graphene layers derived from metal-organic-frameworks as multi-functional electrocatalyst

Yue Wang,[a,b] Kaiyue Li,[a] Feng Yan,[a] Chunyan Li,[a] Chunling Zhu,[b] Xitian Zhang[c] and Yujin Chen[a*]*

[a]*Key Laboratory of In-Fiber Integrated Optics, Ministry of Education and College of Science, Harbin Engineering University, Harbin 150001, China. E-mail: chenyujin@hrbeu.edu.cn.*
[b]*College of Materials Science and Chemical Engineering, Harbin Engineering University, Harbin 150001, China.*
[c]*Key Laboratory for Photonic and Electronic Bandgap Materials, Ministry of Education,and School of Physics and Electronic Engineering, Harbin Normal University, Harbin 150025, China*

*Corresponding authors.

E-mail address es: chenyujin@hrbeu.edu.cn and zhuchunling@hrbeu.edu.cn

EXPERIMENTAL SECTION

1. Materials and Methods.

Ammonium molybdate ($(NH_4)_6Mo_7O_{24} \cdot 4H_2O$) was purchased from Tianjin Kemio Chemical Reagent Co., Ltd. 2-methylimidazole ($C_4H_6N_2$), ethanol (CH_3CH_2OH) and methanol (CH_3OH) were purchased from Tianjin Guangfu Fine Chemical Co., Ltd. Zinc nitrate hexahydrate ($Zn(NO_3)_2 \cdot 6H_2O$) was purchased from Tianjin bodi chemical Co., Ltd. And Cobalt nitrate hexahydrate ($Co(NO_3)_2 \cdot 6H_2O$) was purchased from Shanghai vokai biotechnology Co., Ltd. Poly(vinylpyrrolidone) (PVP) was purchased from Sigma-Aldrich. Hydrogen peroxide (H_2O_2, 30%) was purchased from TianDa Chemical Reagent Co., Ltd. Nitric acid (HNO_3, 65% ~ 68%) was purchased from Xilong Scientific Co., Ltd. Commerical IrO_2 and 20 wt% Pt/C catalysts were purchased from Macklin Biochemical Co., Ltd (Shanghai, China). Nafion solution (5 wt%) was obtained from DuPont Company. All reagents were used directly without further purification and all aqueous solutions were using ultrapure water (> 18.2 MΩ).

2. Synthesis of Mo$_2$C@NC/Co@NG

The MoO_3 nanorods were synthesized according to the previously reported method.[S1, 2] Typically, 34 mg of prepared MoO_3 nanorods was dissolved in 30 mL methanol. After the MoO_3 uniformly dispersed, 210 mg of PVP was dispersed in the solution and ultrasonic 30 min to mix well. The mixture solution was mixed with 300 mg $Zn(NO_3)_2 \cdot 6H_2O$ and 582 mg $Co(NO_3)_2 \cdot 6H_2O$, then the solution was stirred for about 1h to form a clear solution. Subsequently, 982 mg of 2-methylimidazole was dissolved in 10 mL of methanol to form a clear solution and was slowly added into the above solution under stirring. Being kept stirring for 8h, the purple precipitate was collected by centrifugation, washed thoroughly with methanol several times and finally dried in a vacuum drying oven. The as-prepared product was annealed in Ar atmosphere at a given temperature for 2 h with the heating rate of 2 °C min^{-1}. The pyrolysis treatment performed at 800, 900 and 1000 °C were denoted as Mo$_2$C@NC/Co@NG-800, Mo$_2$C@NC/Co@NG-900, Mo$_2$C@NC/Co@NG-1000,

respectively.

3. Synthesis of Mo$_2$C@NC

The synthesis procedure of Mo$_2$C@NC is similar to that of Mo$_2$C@NC/Co@NG-900, expect that without the Co(NO$_3$)$_2$·6H$_2$O.

4. Synthesis of Co@NG

Co@NG nanocrystals were synthesized under the same conditions in the absence of MoO$_3$.

5. Materials Characterization

The powder X-ray diffraction (XRD) patterns were recorded on a Panalytical X-pert diffractometer with Cu Kα radiation (λ=1.5418 Å). The morphology and composition of the electrocatalysts were analyzed by scanning electron microscopy (SEM) (Hitachi SU70), and transmission electron microscopy (TEM) (FEI Tecnai-F20 transmission electron microscope). The compositional depth profile was acquired by using X-ray Photoelectron Spectroscopy (XPS, Themofisher Scienticfic Company) with Al Kα radiation. Brunauer–Emmett–Teller (BET) surface area and pore distribution employed on a Tristar II 3020 gas adsorption analyzer at 77 K.

6. Electrochemical Measurements

3.0 mg of prepared catalysts or commercial 20 wt.% Pt/C catalyst were dispersed in 450.0 mL ethanol with 50.0 mL 5 wt.% Nafion by sonication for at least 5 h to obtain the homogeneous dispersion. Then, the dispersion was dropped onto the rotating disk electrode (RDE, 5 mm diameter, 0.196 cm^2 geometric surface areas) with loading about of 0.18 mg cm^{-2}. A saturated Ag/AgCl electrode was used as the reference electrode and a graphite rod was used as the counter electrode. For the ORR at an RDE, the scanned cathodically at a rate of 10 mV s^{-1} with varying rotating speed from 400 to 2025 rpm in O$_2$-saturated 0.1 M KOH aqueous solution, and the OER was test at 1600 rpm in same conditions.

Koutecky-Levich plots:

The kinetics parameters of ORR can be analyzed using the Koutecky-Levich (K-L) equation and the number of electrons transferred (n) is calculated from the following equations1, 2.shown as follows:

$$\frac{1}{j} = \frac{1}{j_k} + \frac{1}{j_L} = \frac{1}{j_k} + \frac{1}{Bw^{1/2}}$$

(1)

$$B = 0.2nFD_0^{2/3}v^{-1/6}C_0$$

(2)

where j is the measured current density, j_k is the kinetic current density, j_L is the diffusion limiting current, ω is the rate of electrode rotation in rpm, B is Levich slope, n is the number of electron transfers per O_2 molecule, F is the Faraday constant (96485 C mol^{-1}), C_0 is the bulk oxygen concentration in 0.1 M KOH (1.2×10^{-6} mol cm^{-3}), D_0 is the oxygen diffusion coefficient in 0.1 M KOH (1.9×10^{-5} cm^2 s^{-1}), and v is the kinematic viscosity of the electrolyte (0.0109 cm^2 s^{-1}).

The HER activities were determined with a CHI760E electrochemical workstaion in the 1.0 M KOH aqueous electrolyte with a standard three-electrode electrochemical cell. Prepared catalysts, Pt/C (20 wt.%) and IrO_2 were made into working electrodes as follows: the catalyst powder was dispersed in N-methyl-2-pyrrolidone solvent containing 7.5 wt% Poly(vinylidene fluoride) (PVDF) under constantly stirring. The weight ratio of the catalyst to PVDF was 8: 1. Then the mixture was coated onto a piece of carbon paper. The amount of the catalysts on the carbon paper was about 1.0 mg cm^{-2}.A saturated Ag/AgCl electrode was used as the reference electrode and a graphite rod was used as the counter electrode. The polarization curves obtained using linear sweep voltammetry (LSV) at a scan rate of 2 mV s^{-1}. Electrochemical impedance spectroscopy (EIS) measurements were performed by applying an AC voltage with 5 mV amplitude in a frequency range from 0.01 Hz to 100 kHz. The chronopotentiometric measurements were used to assess the long-term stability of the electrocatalysts. All potentials measured were calibrated to reversible hydrogen electrode (RHE) using the following equation: $E_{RHE} = E_{Ag/AgCl} + 0.21 + 0.059 \times pH$. Overpotential ($\eta$) was calculated using the following formula: η (V) $= E_{RHE} - 1.23$ V. All LSV curves reported in this work are corrected by iR loss according to the following formula: $E_{compensated} = E_{measured} - iR$, where $E_{compensated}$ is the compensated potential, $E_{measured}$ the measured potentials and R the equivalent series resistance that was determined by the current interrupt technique.

7. Liquid Zn–air battery assembly

For the liquid Zn-air, 1 mg of catalyst powder and 20 μL of 5 wt% Nafion solution were dissolved in ethanol with at least 30 min sonication to form a homogeneous ink. Then the pre-prepared catalyst ink was coated uniformly onto a hydrophobic carbon paper electrode with a catalyst loading of 1.0 mg cm^{-2} as air electrode. A polished zinc metal plate with thickness of 0.25 mm and width of 4.5 cm was used as the anode. Home-made electrochemical cells were assembled as aqueous primary zinc-air batteries with 6.0 M KOH as the electrolyte, while the rechargeable aqueous zinc-air batteries were prepared with addition of 0.2 M Zn(CH$_3$COO)$_2$ into the above electrolyte.

8. All Solid-state Zn-air battery assembly

The gel electrolyte was prepared as follows: 5 g polyvinyl alcohol (PVA-1788) powder was dissolved in 50.0 mL deionized water at 90 °C under stirring for 2 h to form the clear solution. Then 5 mL solution containing 18 M KOH and 0.02 M Zn(CH$_3$COO)$_2$ was added into the above solution. The mixed solution kept stirring at 90 °C to form homogeneous viscous without bubbles. Finally, Pour the electrolyte solution in the square plastic groove and freezed at -10 °C for over 12 h, then thawed at room temperature. To assemble the all-solid-state Zn-air battert, a polished zinc plate and a carbon fiber cloth substrate (1.5 × 3 cm^2) with 1 mg cm^{-2} catalyst were placed on opposite sides of the polymer electrolyte, follwed by the nickel foam on the ambient dried catalyst layer as current collector. Finally, a polymer film and tapes were used to assemble the solid-state Zn-air battery.

Zinc-air battery tests: All Zn-air batteries were evaluated under ambient conditions. The polarization curves were recorded by linear sweep voltammetry at a scan rate of 10 mV s^{-1} on a CHI760E electrochemical platform. The energy density was calculated based on the applied current (I), average discharge voltage (V), service time (t), and weight of zinc consumed (w_{zn}) as in the following equation:

$$Energy\ density\ (Wh\ kg^{-1}) = \frac{I*V*t}{w_{zn}}$$
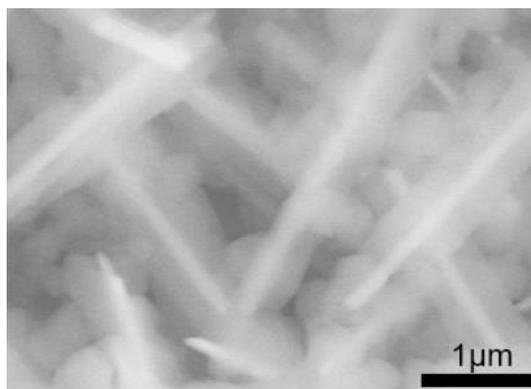
Fig. S1 SEM image of MoO$_3$/CoZn-ZIF.
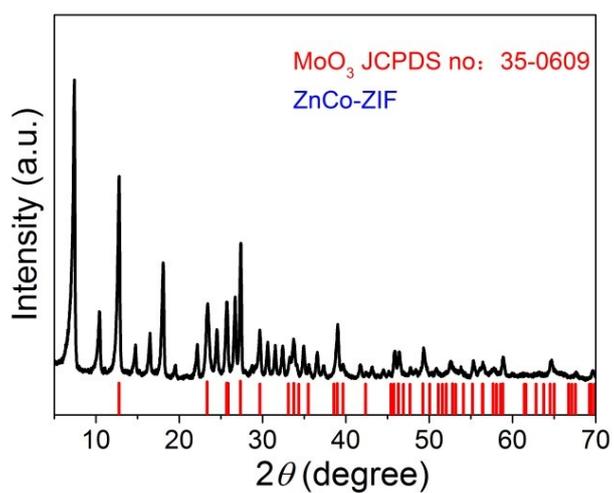
Fig. S2 XRD pattern of MoO$_3$/CoZn-ZIF precursor.
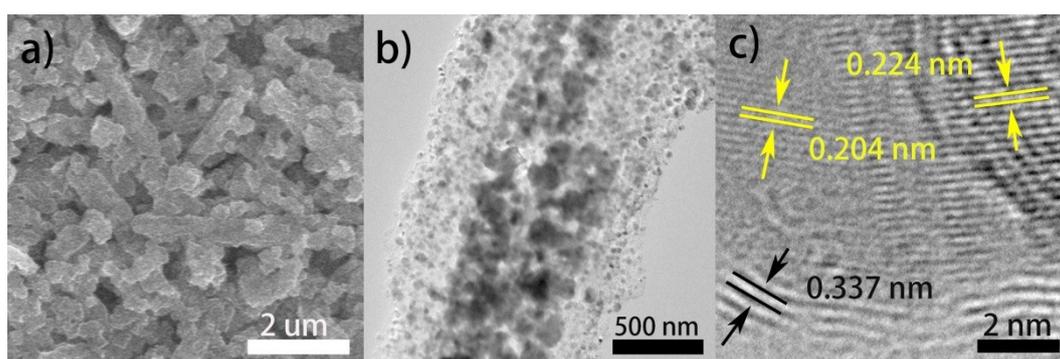
Fig. S3 a) SEM, b) TEM, c) HRTEM images of Mo$_2$C@NC/Co@NG-800.
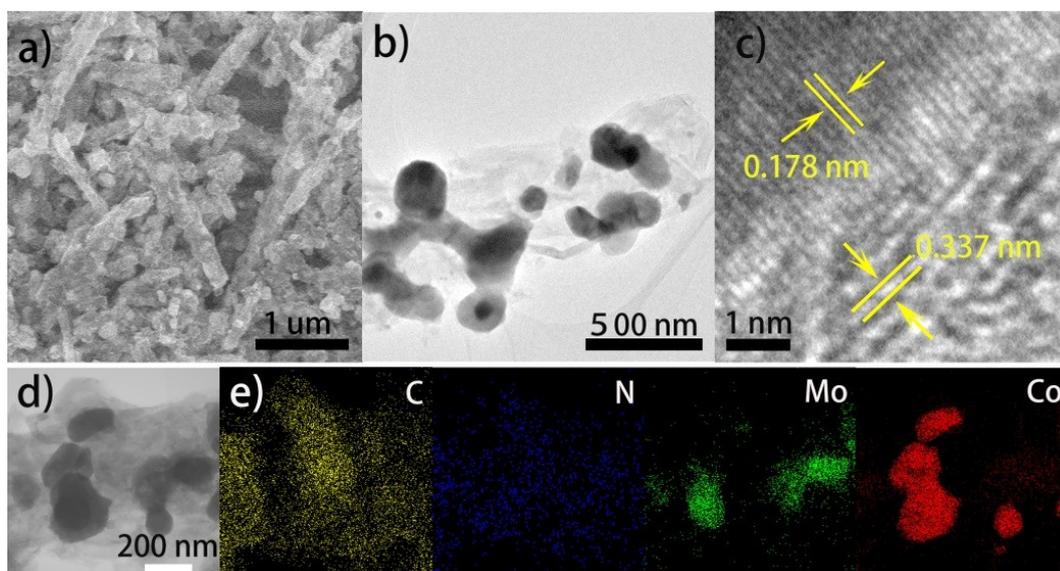
Fig. S4 a) SEM, b) TEM, c) HRTEM, d) TEM images, and e) EDX element mappings of Mo$_2$C@NC/Co@NG-1000.
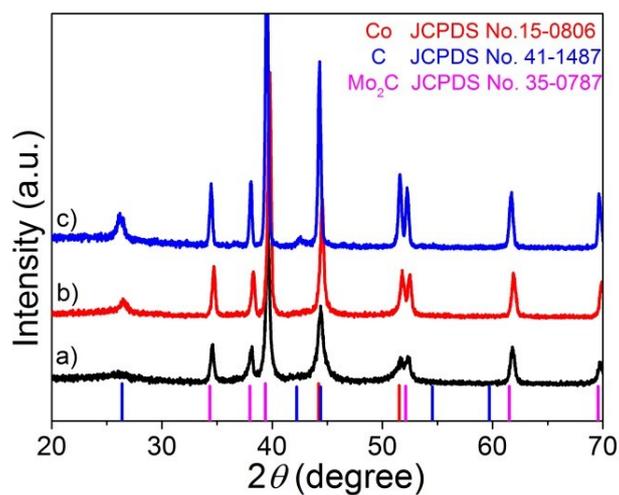
Fig. S5 XRD pattern images of a) Mo$_2$C@NC/Co@NG-800, b) Mo$_2$C@NC/Co@NG-900, and c) Mo$_2$C@NC/Co@NG-1000.
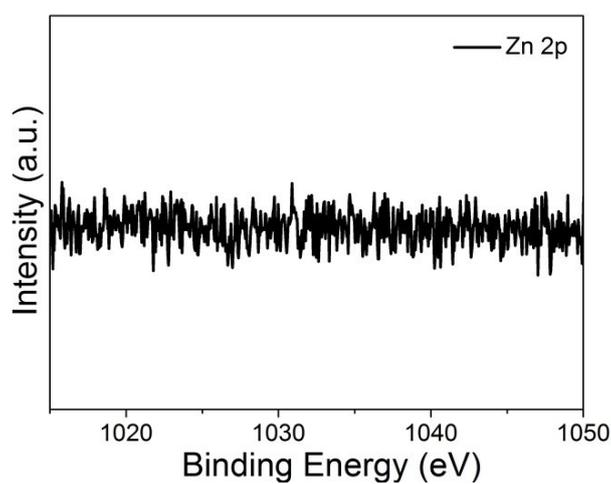
Fig. S6 Zn 2p spectrum of Mo$_2$C@NC/Co@NG catalyst.
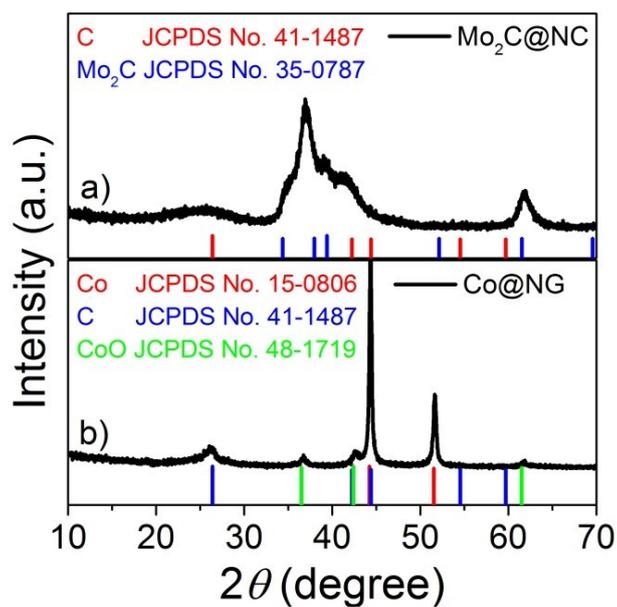
Fig. S7 XRD pattern image of a) Mo$_2$C@NC, and b) Co@NG.
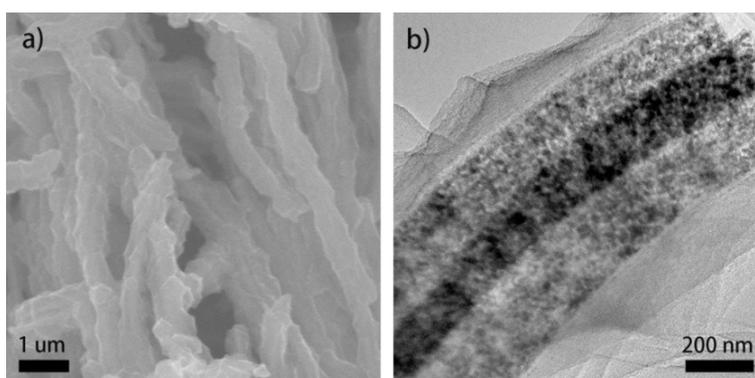
Fig. S8 a) SEM and b) TEM images of the Mo$_2$C@NC.
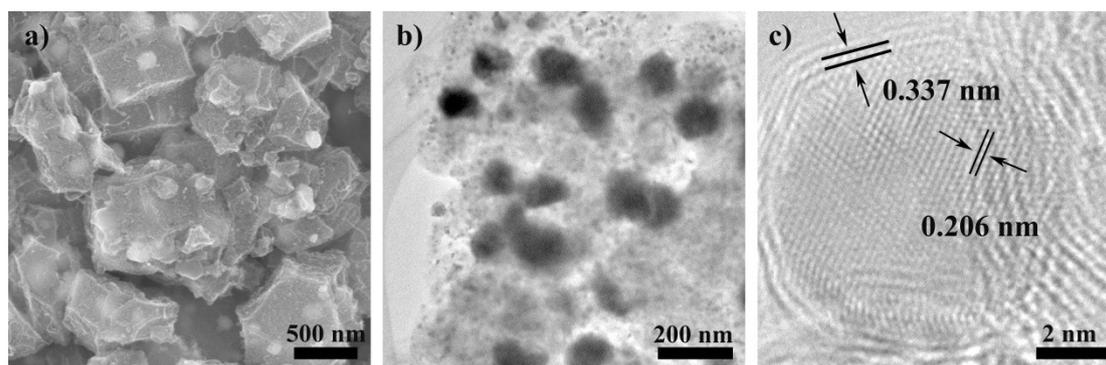
Fig. S9 a) SEM, b) TEM and c) HRTEM images of the Co@NG.
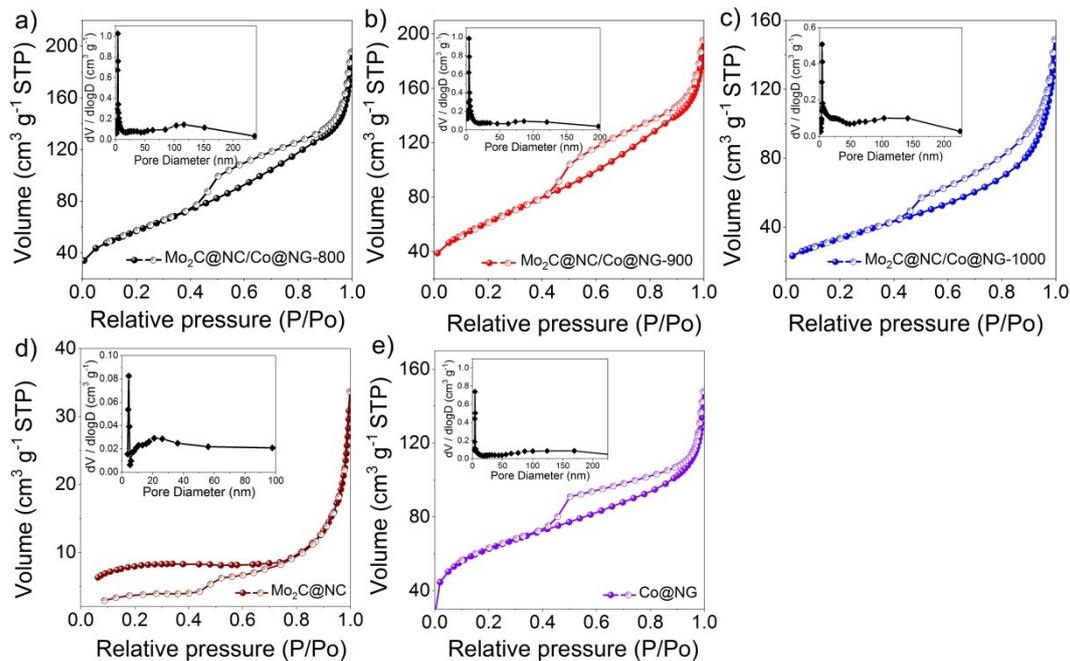
Fig. S10 Nitrogen adsorption/desorption isotherms of a) $Mo_2C@NC/Co@NG$-800, b) $Mo_2C@NC/Co@NG$-900, c) $Mo_2C@NC/Co@NG$-1000, d) $Mo_2C@NC$, and e) $Co@NG$. The insets show the corresponding BJH pore size distributions.
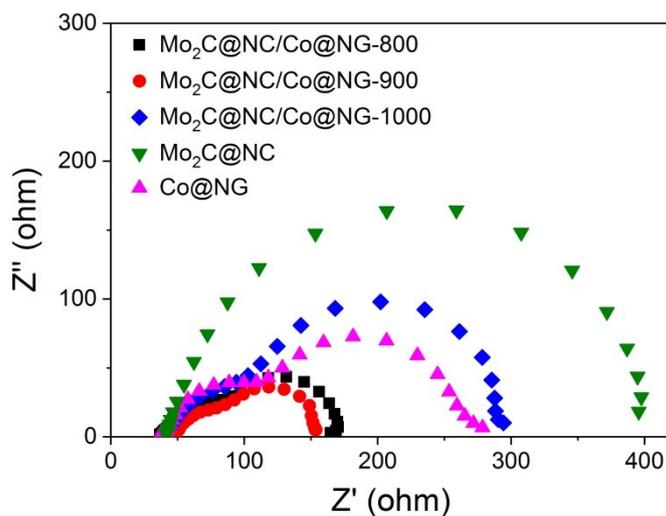
Fig. S11 The Nyquist impedance plots of $Mo_2C@NC/Co@NGs$, $Mo_2C@NC$ and $Co@NG$ in 0.1 M KOH solution.
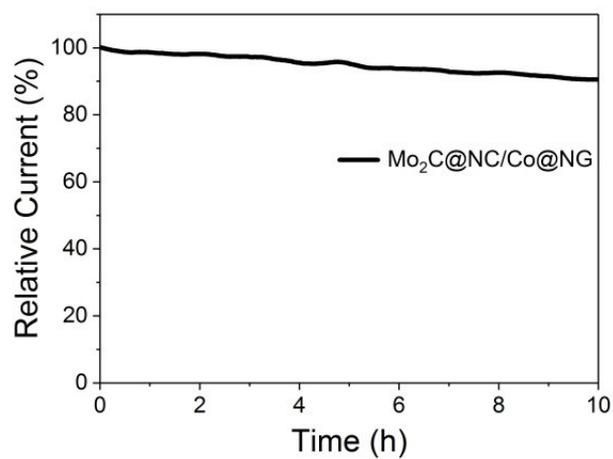
Fig. S12 The stability of Mo$_2$C@NC/Co@NG-900 toward ORR at a given potential of 0.5 V in O$_2$-saturated 0.1 M KOH.
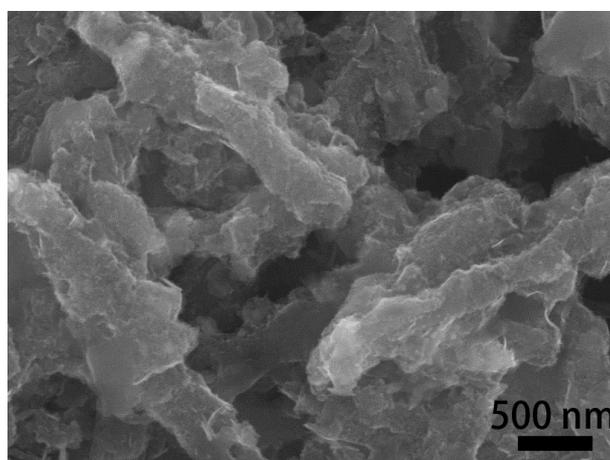
Fig. S13 SEM image of Mo$_2$C@NC/Co@NG-900 electrode after the ORR stability measurement.
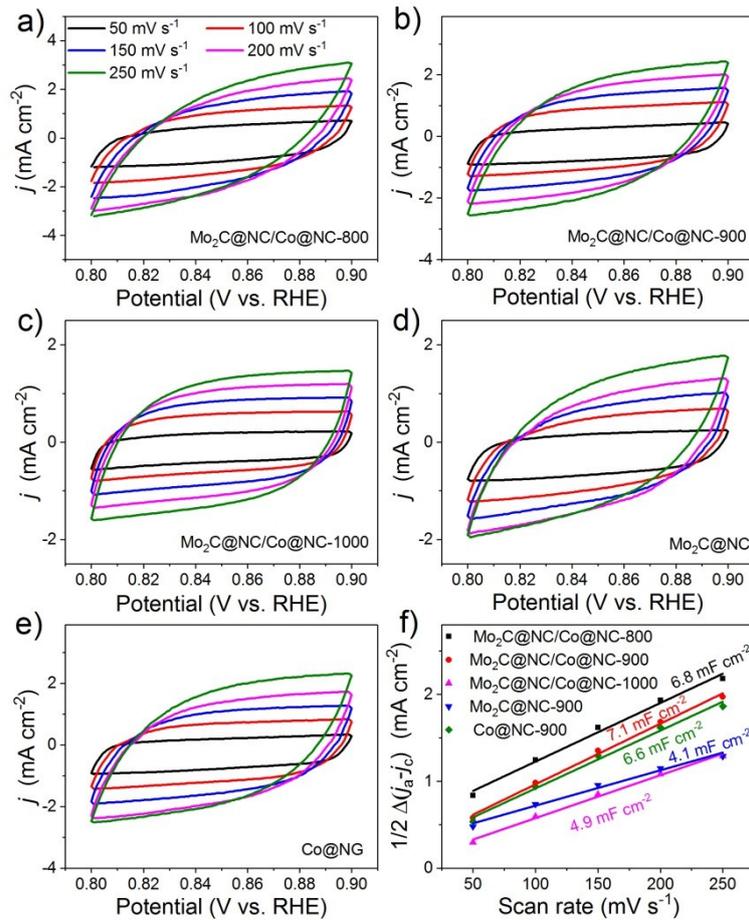
Fig. S14 CV curves of a) Mo$_2$C@NC/Co@NG-800, b) Mo$_2$C@NC/Co@NG-900 c) Mo$_2$C@NC/Co@NG-1000, d) Mo$_2$C@NC, e) Co@NG measured at various scanning rates, respectively. f) Plots of 1/2 Δ(j_a-j_c) vs. scan rate of different catalysts.
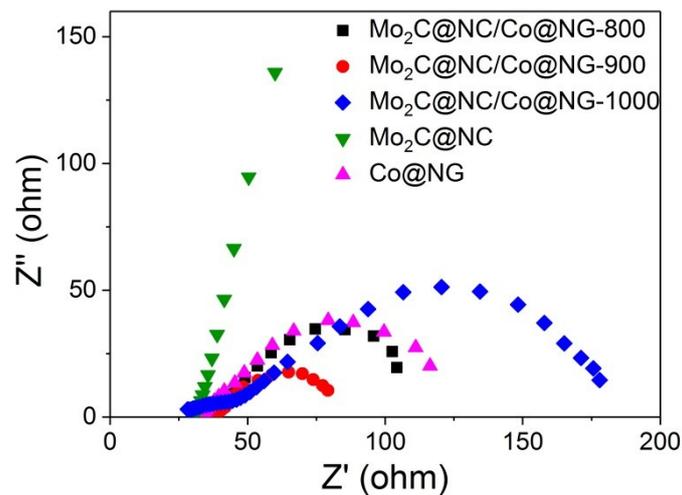
Fig. S15 The Nyquist impedance plots of Mo$_2$C@NC/Co@NGs, Mo$_2$C@NC and Co@NG in 0.1 M KOH solution.
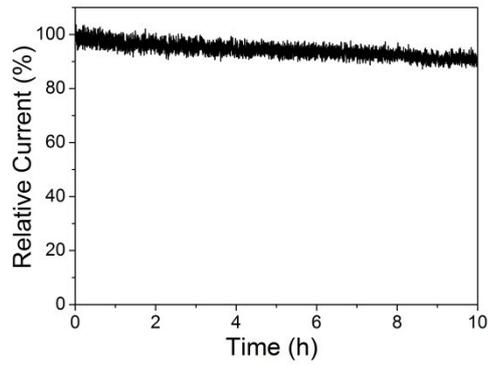
Fig. S16 Durability of Mo$_2$C@NC/Co@NG-900 for OER in 0.1 M KOH.
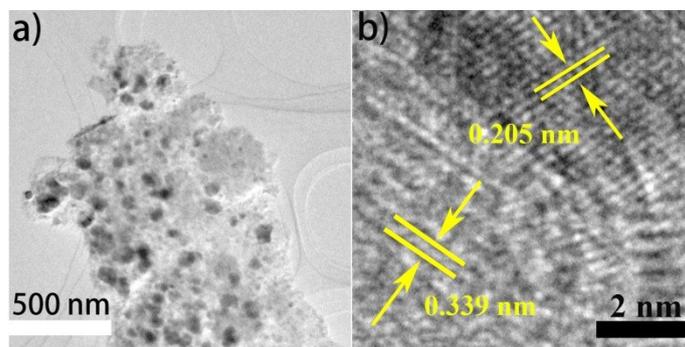
Fig S17 a) TEM and b) HRTEM images of Mo$_2$C@NC/Co@NG-900 electrode after OER testing.
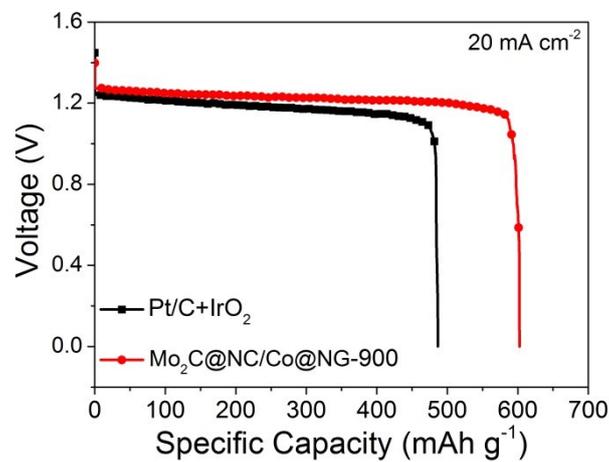
Fig. S18 Specific capacities of the primary Zn-air batteries normalized to the mass of the consumed Zn at the current density of 20 mA cm^{-2}.
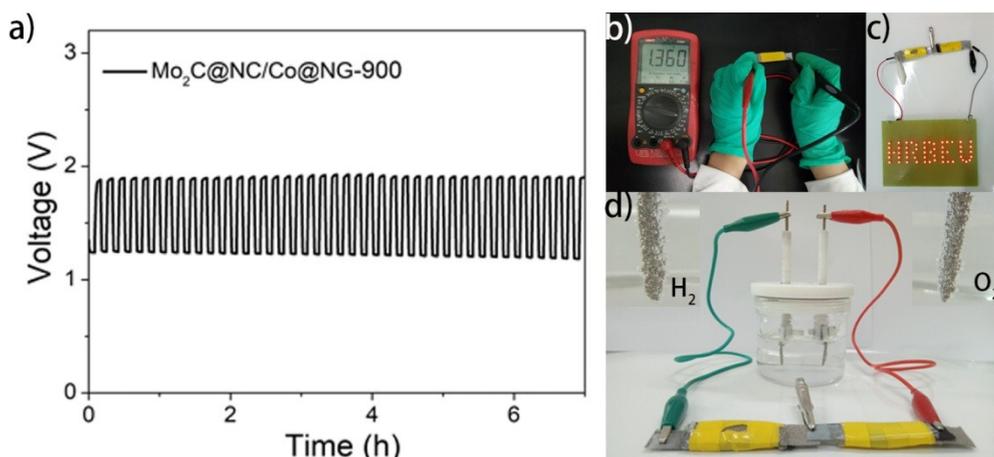
Fig. S19 a) Galvanostatic cycling profiles of Mo₂C@NC/Co@NG-900 based all-solid-state Zn–air battery at the current density of 2 mA cm⁻², b) Photograph of a Mo₂C@NC/Co@NG-900 based all-solid-state Zn–air battery with an open-circuit voltage of 1.360 V, c) Photograph of 55 red LED powered by two all-solid-state Zn-air batteries with the Mo₂C@NC/Co@NG-900 air-cathode in series, d) Photograph of the two-electrode electrolyser powered by two all-solid-state Zn-air batteries with the Mo₂C@NC/Co@NG-900 air-cathode in series. The insets show visible gas bubbles on the electrode surfaces.
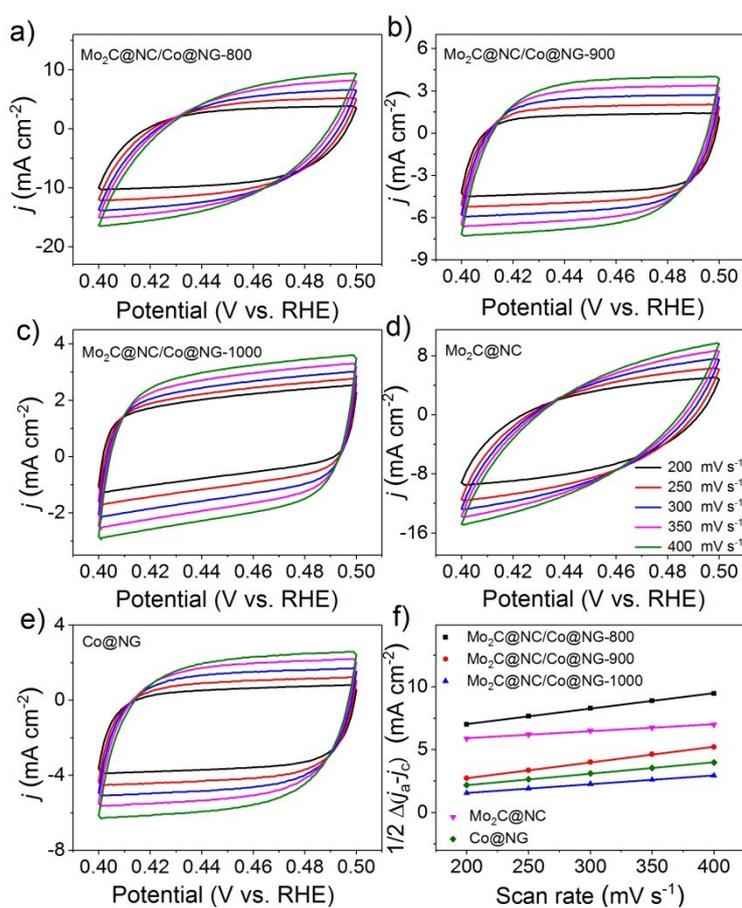
Fig. S20 CV curves measured at various scanning rates of a) Mo₂C@NC/Co@NG-800, b) Mo₂C@NC/Co@NG-900, c) Mo₂C@NC/Co@NG-1000, d) Mo₂C@NC, and e) Co@NG. f) The plots of 1/2 Δ(*j*ₐ-*j*c) vs. scan rate of different catalysts.
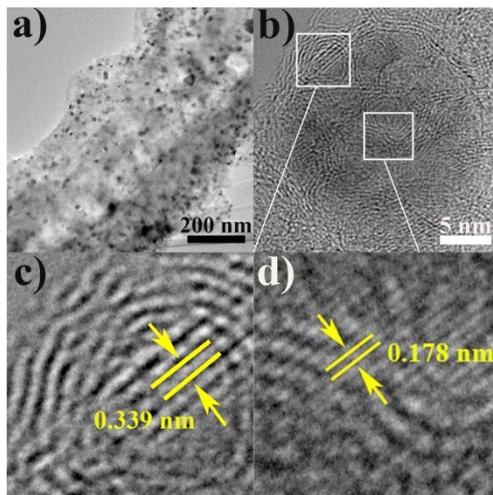
Fig. S21 a,b) TEM images and c,d) HRTEM images of $Mo_2C@NC/Co@NG-900$ electrode after HER process.

Table S1 Nitrogen contents in the $Mo_2C@NC/Co@NG-900$ and Co@NG.

Catalyst	Pyridinic-N (at%)	Co-N (at%)	Pyrrolic-N (at%)	Graphitic-N (at%)	Total (at%)
$Mo_2C@NC/Co@NG-900$	2.59	1.59	0.86	1.29	6.33
Co@NG	0.93	1.01	0.85	0.64	3.43

Table S2. Comparison of ORR catalytic performances of $Mo_2C@NC/Co@NG-900$ with those of other reported catalysts in alkaline mediain 0.1 M KOH (rotating speed : 1600 rpm).

Catalysts	E_{oneset} (V vs. RHE)	$E_{1/2}$ (V vs. RHE)	Ref.
$Mo_2C@NC/Co@NG-900$	0.922	0.867	This work
Mo–N/C@MoS2	0.9	0.81	1
NCNT/CoO-NiO-NiCo	1.0	0.83	8
Fe@C-NG/NCNTs	0.93	0.84	12
Co_4N/CNW/CC	--	0.80	13
CoNC-CNF-1000	--	0.8	16
Carbon-L	0.8610	0.6972	22
Co/NC	--	0.83	25
Co@NC	0.90	0.78	26
3D Co/NCNTs-Zn/Co	0.969	0.841	29
Co/N-BCNT	--	0.83	30
Mo_2C-GNR	0.93	0.81	40
NC@Co-NGC DSNCs	0.92	0.82	41
Co@N-PCF-3	0.92	0.83	45

Table S3. Comparison of OER performance of Mo$_2$C@NC/Co@NG-900 with that of other reported catalysts in 0.1 M KOH electrolyte.

Catalysts	η(V) at j=10 mA cm^{-2}	Ref.
Mo2C@NC/Co@NG-900	1.654	This work
NCNF-1000	1.84	3
Fe@C-NG/NCNTs	1.68	12
CoNC-CNF-1000	1.68	16
Co/NC	1.69	25
Co@NC	1.71	26
NGM-Co	1.74	S3
ZnCo$_2$O$_4$/N-CNT	0.43	S4

Table S4: Comparison of energy storage properties of the primary Zn-air batteries based on of Mo$_2$C@NC/Co@NG-900 with those of ones based other catalysts reported previously.

ORR catalyst used	Open Cricuit Voltage (V)	Peak Power Density (mW cm^{-2})	Specific Capacity (mAh g^{-1})	Ref.
Mo2C@NC/Co@NG-900	1.44	172.1	624	This work
NCNF-1000	1.48	185	626	3
Fe@C-NG/NCNTs	1.44	146.5	682	12
NC@Co-NGC DSNCs	1.45	109	565	41
ZnCo$_2$O$_4$/N-CNT	1.47	82.3	428	S4
CoZn-NC-700	1.42	152	578	S5

S1. L. Fang, Y. Y. Shu, A. Q. Wang and T. Zhang, *J. Phys. Chem. C,* 2007, **111**.

S2. Q. Wang, Z. Lei, Y. Chen, Q. Ouyang, P. Gao, L. Qi, C. Zhu and J. Zhang, *J. Mater. Chem. A*, 2013, **1**, 11795.

S3. C. Tang, B. Wang, H. F. Wang and Q. Zhang, *Adv. Mater.*, 2017, **29**,1703185.

S4. Z.-Q. Liu, H. Cheng, N. Li, T. Y. Ma and Y.-Z. Su, *Adv. Mater.*, 2016, **28**, 3777-3784.

S5. B. H. Chen, X. B. He, F. X. Yin, H. Wang, D.-J. Liu, R. X. Shi, J. N. Chen and H. W. Yin, *Adv. Funct. Mater.,* 2017, **27**, 1700795.